JOURNAL OF MATERIALS SCIENCE 31 (1996) 707–711

Secondary carbide precipitation in an 18 wt %Cr–1 wt % Mo white iron

G. L. F. POWELL
CSIRO Division of Manufacturing Technology, P.O. Box 4, Woodville, South Australia 5011
J. V. BEE
Department of Mechanical Engineering, University of Adelaide, South Australia 5005

High chromium (18%) white irons solidify with a substantially austenitic matrix supersaturated with chromium and carbon. The austenite is destabilized by a high-temperature heat treatment which precipitates chromium-rich secondary carbides. In the as-cast condition the eutectic M_7C_3 carbides are surrounded by a thin layer of martensite and in some instances an adjacent thicker layer of lath martensite. The initial secondary carbide precipitation occurs on sub-grain boundaries during cooling of the as-cast alloy. After a short time (0.25 h) at the destabilization temperature of 1273 K, cuboidal $M_{23}C_6$ precipitates within the austenite matrix with the cube–cube orientation relationship. After the normal period of 4 h at 1273 K, there is a mixture of $M_{23}C_6$ and M_7C_3 secondary carbides and the austenite is sufficiently depleted in chromium and carbon to transform substantially to martensite on cooling to room temperature.

1. Introduction

The high chromium white irons based on the ternary Fe–Cr–C alloy are used extensively for applications requiring resistance to abrasive wear [1]. For castings containing 18% Cr (all compositions are given in wt %), a composition producing a slightly hypo-eutectic microstructure is usually used [2]. In the as-cast condition, the microstructure consists essentially of dendrites of austenite in a matrix of a eutectic mixture of austenite and $(Cr, Fe)_7C_3$ [M_7C_3] carbides. For many applications, the castings are heat treated prior to service. This heat treatment ($\sim$1273 K for an 18% Cr white iron) is designed to destabilize the austenite by the precipitation of chromium-bearing secondary carbides. The reduction in the carbon and chromium contents of the austenite results in substantial transformation of the austenite to martensite on cooling to room temperature [1, 3].

It has been suggested by several authors [1, 4, 5] that the secondary carbides *per se* play a role in determining the mechanical properties of heat-treated high chromium white irons. Diesburg and Borik [1] have suggested that precipitated secondary carbides are the cause of a decrease in K_{IC} fracture toughness from 32 MPa $m^{1/2}$ for an austenitic matrix to 21 MPa $m^{1/2}$ for a martensitic plus precipitated secondary carbide matrix in an 18% Cr white iron. Biner [4] failed to detect an increase in K_{IC} fracture toughness in heat-treated 16% Cr white irons as a function of eutectic carbide morphology and concluded that secondary carbide precipitation was the controlling factor. More recently, Powell and Laird [5] have suggested that the non-equiaxed morphology of the precipitated secondary carbides should be considered as a significant factor in assessing the mechanical properties of a heat-treated high chromium white iron.

This paper reports the results of a microstructural study of an as-cast and heat-treated 18% Cr–1% Mo white iron. Light microscopy, scanning electron microscopy (SEM) and transmission electron microscopy (TEM) have been used to determine the identity as well as the nucleation and growth sequence of secondary carbides

2. Experimental procedure

The high chromium white iron studied was a 15 Cr–3 Mo alloy (actual composition 17.7% Cr–1.1% Mo–3.1% C). Full details of composition and heat treatment have been given previously [5], where the alloy was identified as Alloy B. A condensed description of chemical composition and heat treatment is shown in Table I. Light metallography and scanning electron microscopy were performed after etching in Vilella's reagent. Discs for transmission

TABLE I Actual composition of high-chromium alloy iron 15Cr–3Mo, together with contents in the dendritic matrix after heat treatment at 1273 K.

	C (wt %)	Cr (wt %)	Mo (wt %)
Alloy	3.1	17.7	1.1
Dendritic matrix	1.2	10.1	0.4

0022–2461

electron microscopy were prepared by standard techniques and thin foils produced using a twin-jet electropolisher. These samples were examined in a Jeol 2000 FX AEM operating at 200 kV.

3. Results and discussion

3.1. As-cast condition

Fig. 1 shows the microstructure of the as-cast alloy cooled at 0.15 $K s^{-1}$. In this light micrograph, the eutectic carbides are surrounded by a thin dark-etching layer, while the lines of fine secondary carbide precipitate are barely visible. In the scanning electron micrograph (Fig. 2), it can be seen that the eutectic carbides are surrounded by a narrow region in which the austenite has transformed to martensite (due to local carbon and chromium depletion), while fine secondary carbide precipitation has occurred only on sub-grain boundaries. Precipitation on sub-boundaries has also been found after high-temperature destabilization of 19% Cr irons, but only after pre-annealing [6].

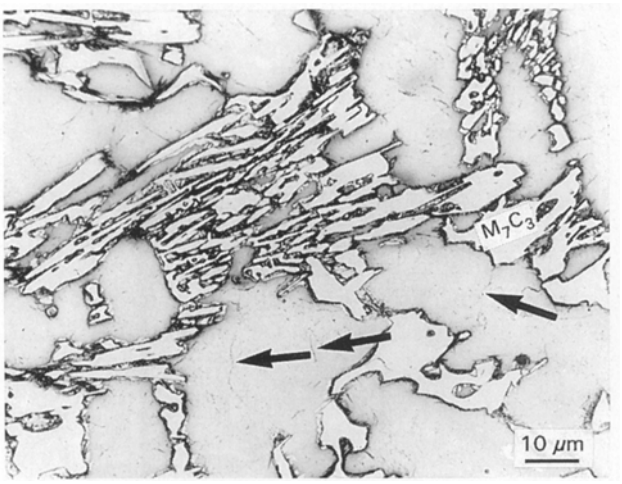

Figure 1 Light micrograph of an alloy in the as-cast condition cooled at 0.15 $K s^{-1}$. Barely visible dark lines of precipitates within the austenitic matrix are marked by arrows. The outlined white constituent is eutectic M_7C_3.

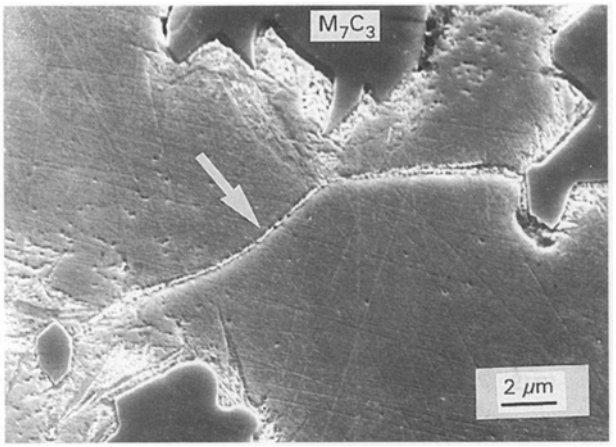

Figure 2 Scanning electron micrograph of fine secondary carbide precipitation on sub-grain boundaries (arrowed) in the as-cast matrix. The eutectic carbides are marked M_7C_3.

Transmission electron microscopy showed that the matrix of the as-cast material was austenitic and contained deformation twins and a high dislocation density (Fig. 3). Although some deformation might be expected from the differential thermal contraction stresses induced during cooling of the eutectic structure, in this case it is more likely the result of damage to the thin foil. Close to the eutectic carbides some transformation was observed, which had the appearance of lath (low-carbon) martensite (marked M in Fig. 4a). A b c c structure was confirmed by selected-area diffraction (Fig. 4b). The transformation of austenite to form a thin rim of martensite adjacent to eutectic carbide (marked L in Fig. 4a) has been reported previously [7]. This was shown to be associated with a local depletion of chromium at the carbide/austenite interface. In the present study, this rim is also present but the further decomposition of austenite to form lath martensite (in a different orientation) indicates a simultaneous local depletion in carbon content.

3.2. Heat-treated condition

Holding at the heat-treatment temperature of 1273 K for only 0.25 h produced significant intragranular precipitation (Fig. 5). Close to the eutectic carbides there is a dense distribution of very fine precipitates. In the centres of the austenite grains, coarser secondary carbide precipitates have a cuboidal morphology and many are aligned in rows to form a grid. Transmission

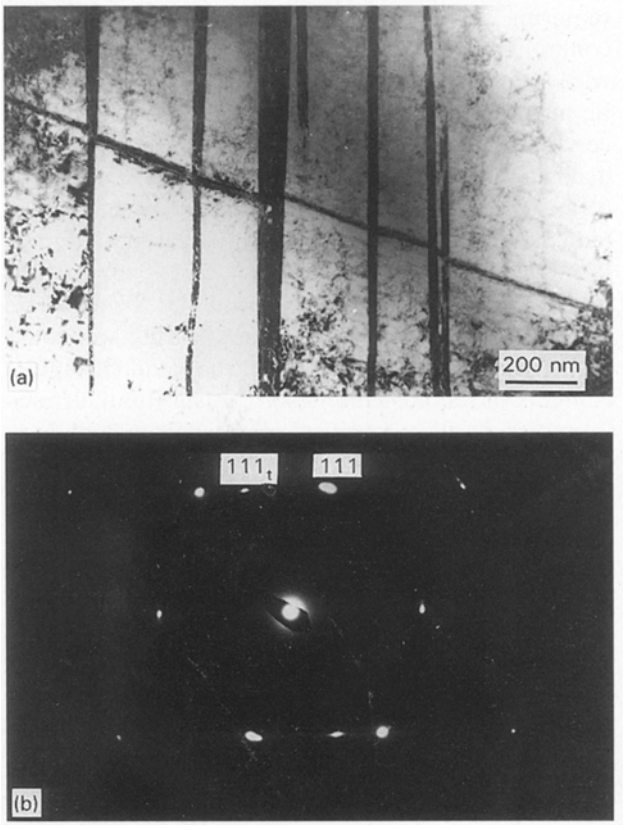

Figure 3 (a) Transmission electron micrograph showing the austenitic matrix of the as-cast material, containing deformation twins. (b) SADP from the region shown above, showing a ⟨1 1 0⟩ f c c zone axis and a {1 1 1} twin reflection.

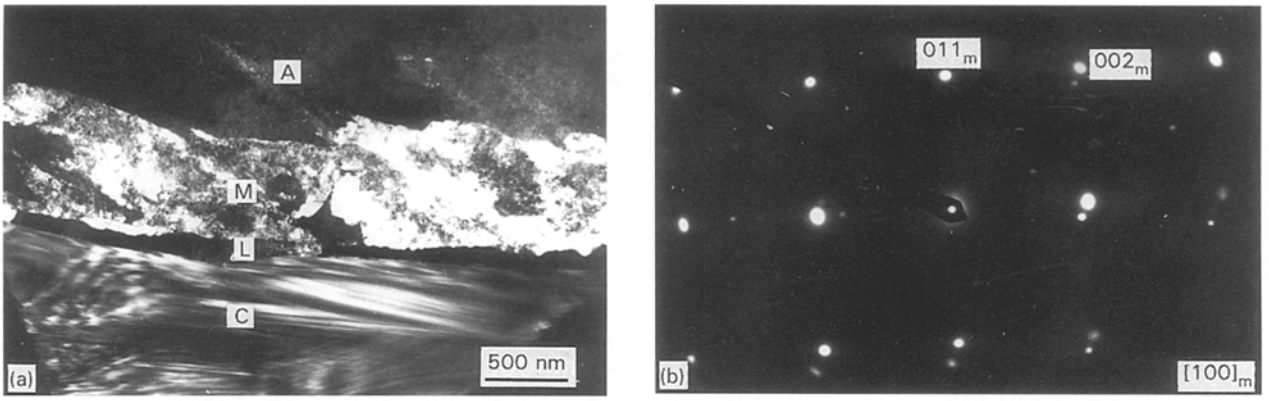

Figure 4 (a) A centred dark-field transmission electron micrograph of the lath martensitic matrix (M) close to a eutectic carbide (C) in as-cast material. Another thin martensitic area (L) immediately adjacent to the carbide has not been illuminated. The remaining matrix (A) was identified as austenite. (b) SADP of the lath martensitic phase shown above.

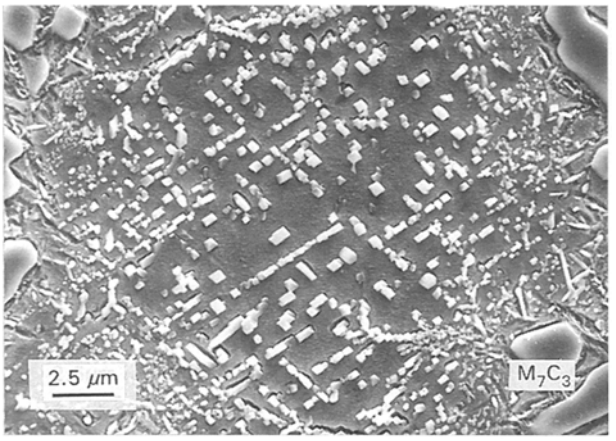

Figure 5 Scanning electron micrograph showing a grid of secondary carbides after 0.25 h at 1273 K.

electron microscopy revealed that these precipitates contained faults (Fig. 6a and b), while the associated selected-area diffraction pattern identified them as $M_{23}C_6$ with a cube–cube orientation relationship with the austenitic matrix (Fig. 6c). Faulted carbides in chromium-containing alloys are usually indicative of M_7C_3; however, in this material the precipitate was identified as $M_{23}C_6$. The internal structure therefore probably represents annealing twins developed during growth. The formation of $M_{23}C_6$ is unexpected, because according to the equilibrium phase diagram the thermodynamically stable phase is M_7C_3. This behaviour has been observed previously in the annealing of Fe–Cr–C hardfacing alloys [8]. The preferential formation of $M_{23}C_6$ rather than the equilibrium (complex hexagonal) M_7C_3 is explained in terms of the good lattice matching between austenite and $M_{23}C_6$. $M_{23}C_6$ has a lattice parameter almost exactly three times that of austenite and precipitation in the normal cube–cube orientation relationship minimizes the interfacial energy requirements and reduces the activation energy for nucleation.

Even after such a short time at this temperature there is evidence of growth and coalescence of the cuboidal particles (Fig. 7a). Again internal faulting is visible and while the selected-area diffraction pattern (Fig. 7b) still shows a dominant $M_{23}C_6$ structure, there is some evidence of the presence of M_7C_3. This

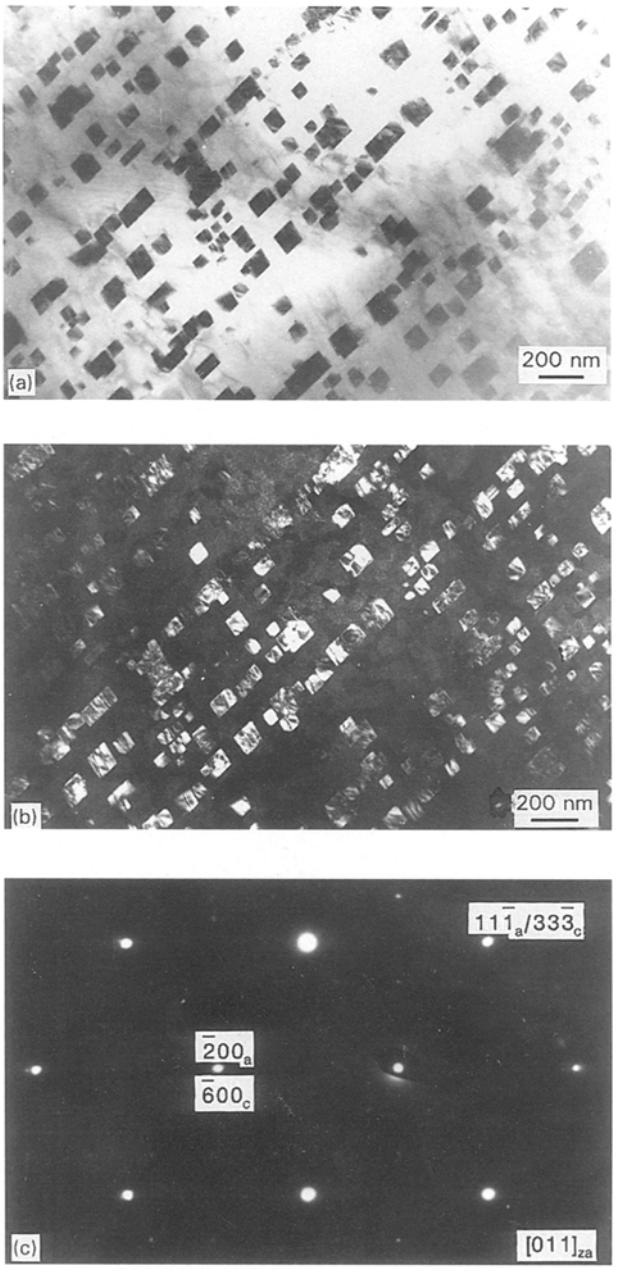

Figure 6 (a) Bright-field transmission electron micrograph of the cuboidal precipitates formed after 0.25 h at 1273 K. (b) Dark-field micrograph of the same region, using a $\{1\,1\,\bar{1}\}M_{23}C_6$ reflection. (c) SADP showing a cube–cube austenite: carbide orientation relationship.

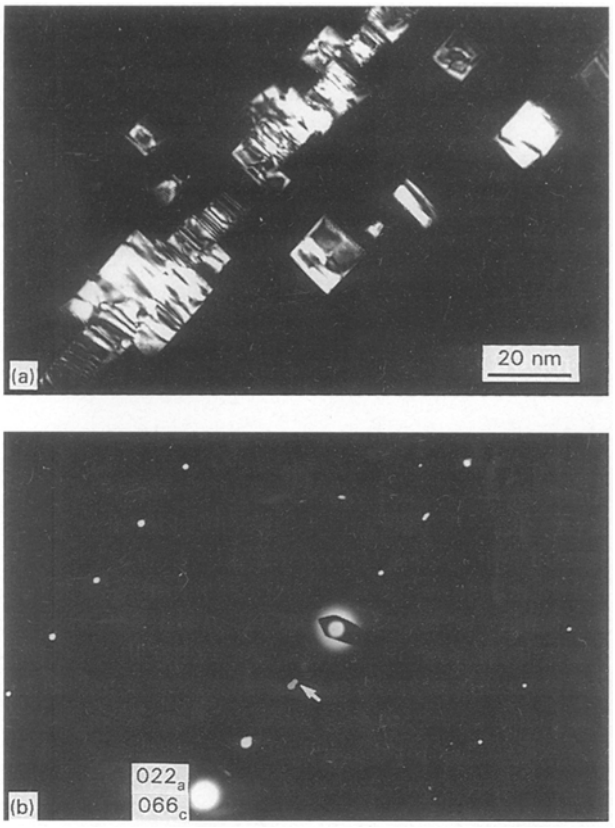

Figure 7 (a) A centred dark-field transmission electron micrograph showing coalescence of cuboidal precipitates after 0.25 h at 1273 K. (b) SADP showing an $M_{23}C_6$ zone and a spot (arrowed) which is consistent with an $\{0\,1\,.\,1\}$ M_7C_3 reflection.

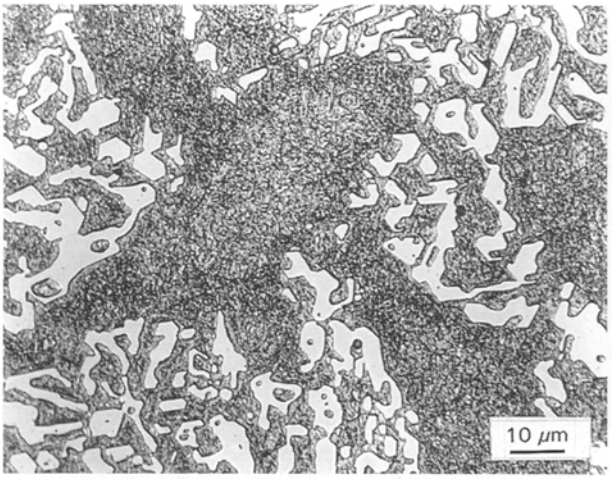

Figure 8 Light micrograph of alloy after 4 h at 1273 K. The secondary carbide precipitate appears as very small outlined white areas.

could be indicative of the start of an *in situ* transformation to the equilibrium carbide phase.

After 4 h at 1273 K, there is copious precipitation of secondary carbides, which appear as small outlined white areas in a dark-etching matrix (Fig. 8). In the SEM, the carbides are revealed as varying in both size and morphology. Large carbides appear as rods or with a hexagonal cross-section (Fig. 9a). The smaller carbides are bounded by orthogonal facets (arrowed in Fig. 9b), which suggests coalescence of the cuboidal precipitates described above.

Transmission electron microscopy revealed that there has been considerable growth of the cuboidal precipitates (Fig. 10a) but most of the interfaces remain planar. Again the selected-area diffraction pattern (Fig. 10b) has a dominant cubic pattern with some evidence of M_7C_3. This suggests great stability and the *in situ* transformation to M_7C_3 cannot be a dominant mechanism. In other areas, precipitate particles containing multiple fine parallel faults were observed in a martensitic matrix (Fig. 11a). These were typically elongated and correspond to the rods seen in

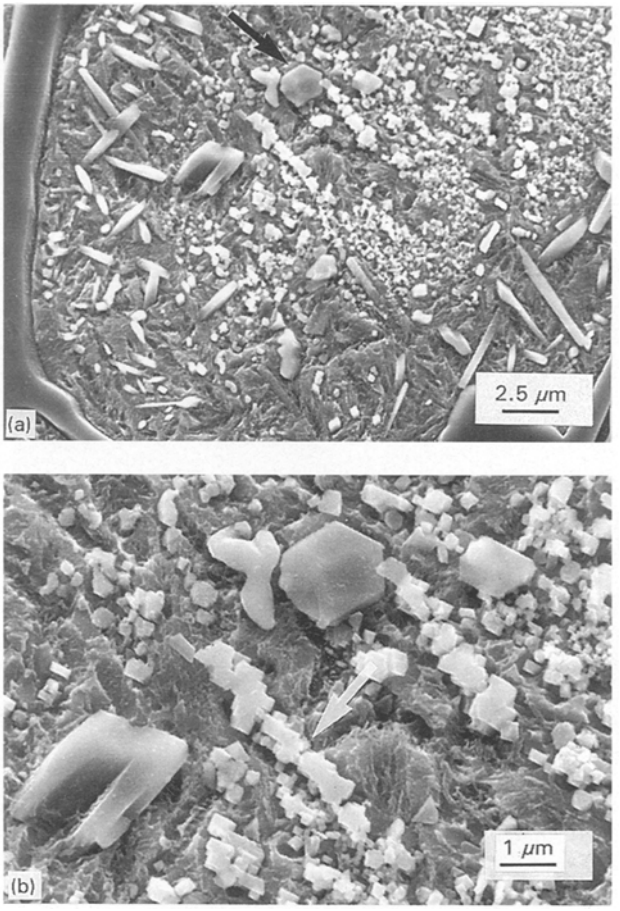

Figure 9 Scanning electron micrographs of the fine secondary carbide precipitate shown as very small white areas in Fig. 8. In (a) large carbides appear as rods or with a hexagonal cross-section. In (b) the smaller precipitates are bounded by facets at right angles (arrowed).

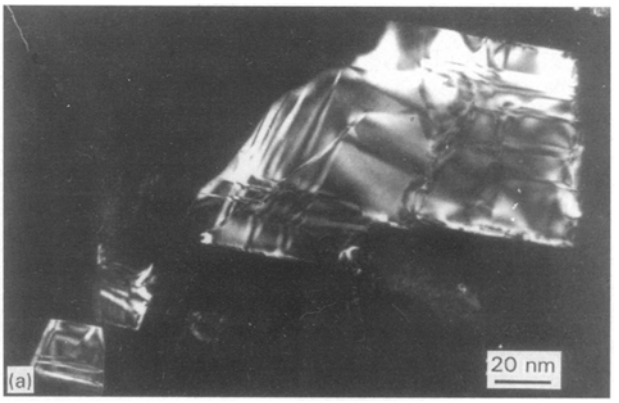

Figure 10 (a) A centred dark-field transmission electron micrograph of a coarse (~1.2 μm) cuboidal precipitate after 4 h at 1273 K, using a $\{1\,1\,3\}$ $M_{23}C_6$ reflection. (b) SADP showing $M_{23}C_6$ and bcc matrix zones, and diffraction spots (arrowed) consistent with the presence of M_7C_3.

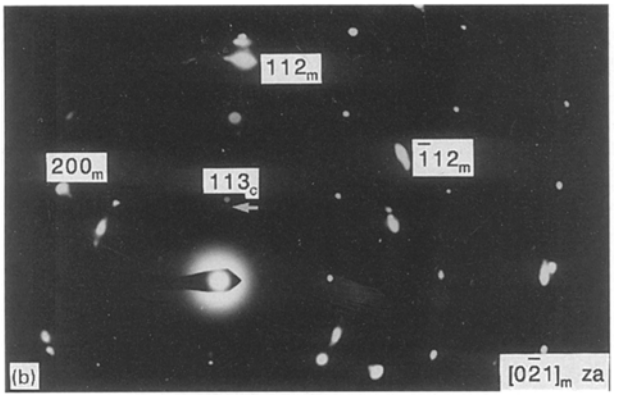

Figure 10 Continued

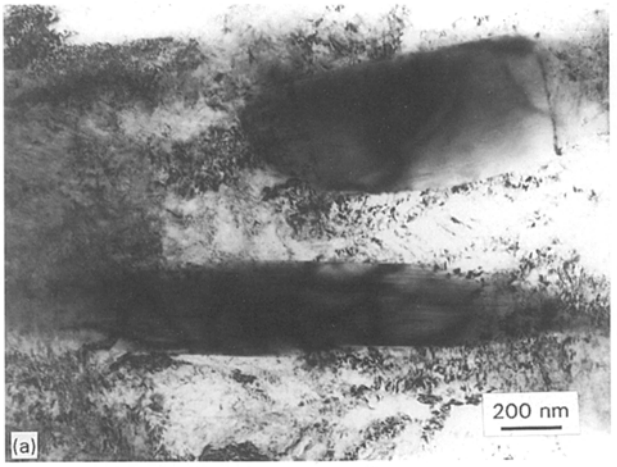

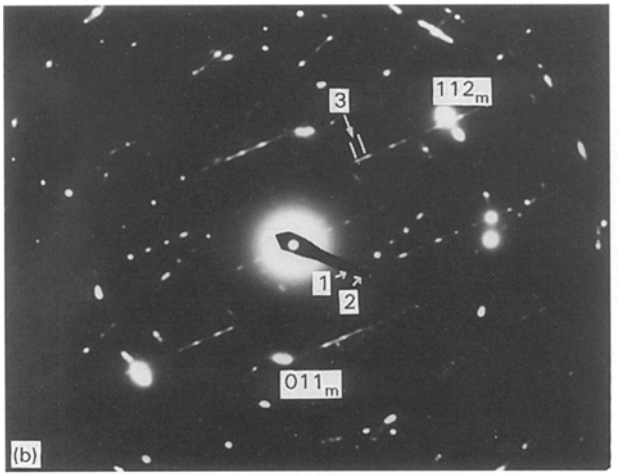

Figure 11 (a) Transmission electron micrograph of rod precipitates in a martensitic matrix. (b) SADP showing strong bcc matrix reflections and two streaked precipitate patterns (arrowed 1, 2) typical of M_7C_3. The periodicity of the precipitate spots (arrowed 3) is consistent with that of $\{0\,1.0\}$ M_7C_3.

the SEM (Fig. 9). The selected-area diffraction pattern from this region was complex (Fig. 11b) but the streaking and periodicity of the diffraction spots is typical of two different orientations of the equilibrium M_7C_3. These were not associated with any cuboidal precipitates and probably formed by a separate nucleation process.

Precipitation is sufficient at this time to destabilize the austenite and the bulk of the matrix was found to be martensitic.

4. Conclusions

1. Local depletion of chromium close to eutectic carbides in the as-cast alloy results in the formation of a thin layer of martensite. The simultaneous depletion in carbon can produce further decomposition of austenite to form a lath martensite.

2. Initial precipitation of secondary carbides occurs on sub-grain boundaries in the austenite matrix of the as-cast material during cooling.

3. A short destabilization heat treatment (0.25 h at 1273 K) produces regular arrays of cuboidal intragranular secondary carbides. These were identified as $M_{23}C_6$ with a cube–cube orientation relationship with the austenite matrix

4. After longer heat treatment (4 h at 1273 K) copious precipitation of $M_{23}C_6$ still exists, but rods of the equilibrium M_7C_3 have also developed. Destabilization is sufficient here to produce a fully martensitic matrix on cooling.

Acknowledgements

The authors thank G. Herfurth and P. Lloyd for light and scanning electron microscopy, respectively, and are grateful for the support of this work through grants from the University of Adelaide/CSIRO collaborative research fund and the Australian Research Council.

References

1. D. E. DIESBURG and F. BORIK, in "Symposium Materials for the Mining Industry", edited by R. Q. Barr (Climax Molybdenum, Vail, USA, 1974) p. 15.
2. R. B. GUNDLACH, *Trans. Am. Foundryman's Soc.* **82** (1974) 309.
3. W. W. CIAS, *ibid.* **82** (1974) 317.
4. S. B. BINER, *Canad. Metall. Q.* **24** (1985) 163.
5. G. L. F. POWELL and G. LAIRD II, *J. Mater. Sci.* **27** (1992) 29.
6. K. A. KIBBLE and J. T. H. PEARCE, *Cast Metals* **6** (1993) 9.
7. G. L. F. POWELL and J. V. BEE, in Proceedings of the Conference on "Materials and Manufacturing in Mining and Agriculture", Brisbane (Institute of Metals and Materials Ltd., Australasia, 1993) p. 21.
8. S. ATAMERT and K. D. H. BHADESHIA, *Mater. Sci. Eng.* **A130** (1990) 101.

Received 10 August 1994
and accepted 15 August 1995